

THE CIRCUMSTELLAR DISK MASS DISTRIBUTION IN THE ORION TRAPEZIUM CLUSTER

RITA K. MANN, JONATHAN P. WILLIAMS

Institute for Astronomy, University of Hawaii, 2680 Woodlawn Drive, Honolulu, HI 96822

(Received 2008 Nov 26)

ACCEPTED TO APJL: 2009 Feb 3

ABSTRACT

We present the results of a submillimeter interferometric survey of circumstellar disks in the Trapezium Cluster of Orion. We observed the 880 μm continuum emission from 55 disks using the Submillimeter Array¹, and detected 28 disks above 3σ significance with fluxes between 6-70 mJy and rms noise between 0.7–5.3 mJy. Dust masses and upper limits are derived from the submillimeter excess above free-free emission extrapolated from longer wavelength observations. Above our completeness limit of $0.0084 M_{\odot}$, the disk mass distribution is similar to that of Class II disks in Taurus-Auriga and ρ Ophiuchus but is truncated at $0.04 M_{\odot}$. We show that the disk mass and radius distributions are consistent with the formation of Trapezium Cluster disks ~ 1 Myr ago and subsequent photoevaporation by the ultraviolet radiation field from θ^1 Ori C. The fraction of disks which contain a minimum mass solar nebula within 60 AU radius is estimated to be 11 – 13% in both Taurus and the Trapezium Cluster, which suggests the potential for forming Solar Systems is not compromised in this massive star-forming region.

Subject headings: circumstellar matter — planetary systems: protoplanetary disks — solar system: formation — stars: pre-main sequence

1. INTRODUCTION

Circumstellar disks are the birth sites of planets, making their fundamental properties, such as mass and size, directly related to the types of planets that can form. Disk masses are most easily measured by observations at millimeter wavelengths, where the dust grain optical depth is less than unity. Surveys of stars with ages $\sim 0.3 - 10$ Myr in the Taurus and ρ Ophiuchus dark clouds show a broad range of disk masses around a median of $0.005 M_{\odot}$ (Andrews & Williams 2005, 2007a), which is within a factor of two required to form our Solar System (the minimum mass solar nebula; MMSN = $0.01 M_{\odot}$ (Weidenschilling 1977)). Most studies to date of disk masses have focused on Taurus and ρ Ophiuchus because they are the nearest star-forming regions. However, most stars do not form in relative isolation as in these regions, but in dense clusters containing high mass stars (Lada & Lada 2003). The Orion Trapezium Cluster is more representative of the typical birthplace of most stars, including our Sun. There are more than 2000 stars with mean ages less than 1 Myr packed within 1 pc^3 in the Trapezium (Hillenbrand 1997). Hubble Space Telescope (HST) images of this region provided the first direct images of circumstellar disks (dubbed “proplyds”), spectacularly seen silhouetted against the bright background (O’Dell & Wen 1994; O’Dell & Wong 1996; Bally et al. 2000). Cometary-shaped cocoons of ionized gas surround many disks, excited by ultraviolet radiation from the most massive and luminous (O6) star at the center of the cluster, θ^1 Ori C (McCullough et al. 1995; Bally et al. 1998a). Centimeter wavelength observations have revealed photoevaporative mass loss rates

of $\dot{M} \sim 10^{-7} M_{\odot} \text{ yr}^{-1}$, which are sufficient to remove a MMSN outside the gravitationally bound radius in ~ 1 Myr (Churchwell et al. 1987; Henney et al. 1999).

Mass loss is expected to be concentrated in the outer parts of the disk with the inner regions potentially surviving longer (Johnstone et al. 1998; Adams et al. 2004; Clarke 2007). But the amount of material in the inner disk regions available to form planets was unknown. Weak lower limits on disk mass exist from the extinction of the central star and background nebula (McCaughrean et al. 1998) but measurements of optically thin disk emission are required for comparison with Taurus and other star-forming regions. Detecting dust emission from disks in the Trapezium Cluster is challenging because of its distance (3 times further than Taurus), the small angular separation between disks, and substantial levels of ionized gas from the surrounding cocoons, which swamp dust emission at centimeter to millimeter wavelengths (Mundy et al. 1995). The Submillimeter Array (SMA) is ideally suited to detecting thermal dust emission from the Trapezium Cluster disks, as it overcomes the above problems with its combination of high sensitivity, high resolution, and high frequency.

We have carried out a survey of HST-identified proplyds in the Trapezium Cluster using the SMA in order to determine the disk mass distribution. We describe the observations in §2, the determination of masses and comparison with Taurus and ρ Ophiuchus in §3, and discuss the implications of our findings for disk evolution and the possibility of planet formation in §4.

2. OBSERVATIONS

Submillimeter interferometric observations at 880 μm were conducted with the SMA on Mauna Kea over 9 nights between 2006-08 (see Figure 1¹). The compact configuration of the 8-element interferometer was chosen

Electronic address: rmann@ifa.hawaii.edu, jpw@ifa.hawaii.edu

¹The Submillimeter Array is a joint project between the Submillimeter Astrophysical Observatory and the Academia Sinica Institute of Astronomy and Astrophysics and is funded by the Smithsonian Institution and the Academia Sinica.

¹ HST image from <http://casa.colorado.edu/~bally/HST/HST/master/>.

to provide the best phase stability, and sufficient resolution ($\sim 2.5''$) to distinguish individual disks. With the exception of the central region around θ^1 Ori C, fields were chosen to lie in regions of relatively low and uniform background cloud emission. Field B was intentionally chosen to overlap the 2004 observations of Williams et al. (2005) because of improvements in array sensitivity.

Observations were carried out during good weather conditions with precipitable water vapor levels below 2 mm, resulting in system temperatures ranging from 100-400 K. Amplitude and phase calibration were performed through observations of the quasars J0423-013 and J0530+135. Passband calibration was conducted with bright quasars 3C454.3, 3C279, or 3C273 and Uranus or Titan were used to set the absolute flux scale, which is estimated to be accurate to $\sim 10\%$.

The Trapezium Cluster has formed a blister HII region and sits in front of a Giant Molecular Cloud. Bolometer maps made with the SCUBA camera on the James Clerk Maxwell Telescope by Johnstone & Bally (1999) show that the cloud produces a strong $850 \mu\text{m}$ background of several Jy per $15''$ beam. This corresponds to $\sim 10 \text{ mJy}$ per square arcsecond and is comparable to disk emission. We produced images using physical baselines greater than 23 m (27λ) to filter extended emission on angular scales $\gtrsim 7''$, which lowered the cloud background substantially but preserved compact emission from the disks. Nevertheless, the background contributed significantly to the noise level in several fields.

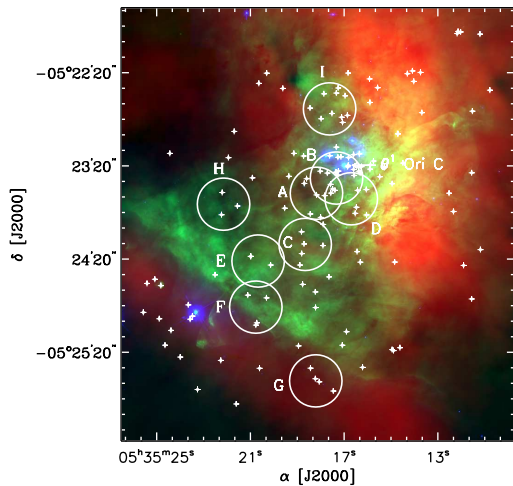


FIG. 1.— Large-scale view of the Orion Trapezium Cluster as a color mosaic of images from the Hubble Space Telescope (HST) and James Clerk Maxwell Telescope (JCMT). JCMT/SCUBA $450 \mu\text{m}$ observations are in red (from Johnstone & Bally (1999)), HST F555W in blue and H α in green². Blue stars near the center of the image are the four OB stars that give the Trapezium its name. The most massive member, θ^1 Ori C, is labelled. Solid circles represent the $32''$ primary beam of each SMA field.

3. RESULTS

3.1. Disk mass determination

The 9 SMA fields include a total of 55 HST-identified disks from the catalogs of O'Dell & Wong

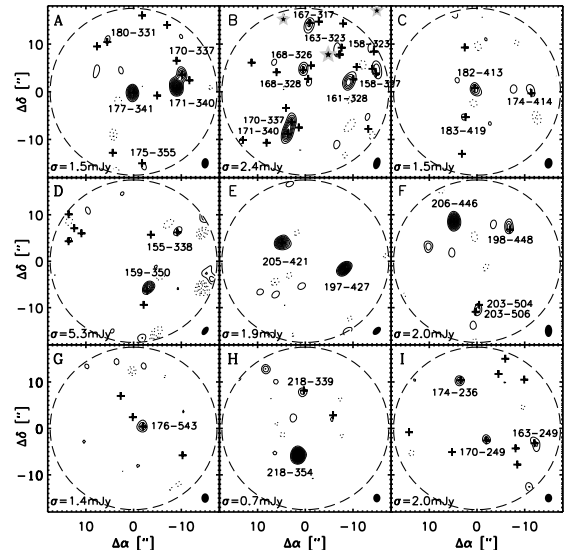


FIG. 2.— Continuum emission at $880 \mu\text{m}$ toward 9 SMA fields. Alphabetical labels correspond to pointings in Figure 1. The 55 HST-identified disks that lie within the $32''$ SMA primary beams (shown as dashed circles) are marked with crosses and the 28 detections are labeled using standard proplyd nomenclature. The OB stars are shown with star symbols in Field B. The contours in each field begin at 3σ and increase by 2σ , where the rms noise level, σ , is specified in the lower left corner of each map. The synthesized beam is shown in the lower right corner of each map.

(1996); Bally et al. (2000); Vicente & Alves (2005) and are shown in Figure 2. We detected 28 disks with a signal-to-noise ratio ≥ 3 and refer to them in the standard proplyd nomenclature (O'Dell & Wen 1994). Given the relatively large beam size ($\sim 1000 \text{ AU}$), all the detections are point sources and we measured their fluxes in a beam-sized aperture centered on the HST position. The observed submillimeter fluxes are composed of 3 components: blackbody emission from the dust in the disks, F_{dust} , free-free emission from the cocoons of ionized gas, F_{ff} , and background cloud emission, F_{bg} :

$$F_{\text{obs}} = F_{\text{dust}} + F_{\text{ff}} + F_{\text{bg}}. \quad (1)$$

The radio-millimeter spectral energy distributions (SED) for each SMA detected disk are shown in Figure 3. The free-free emission from several disks detected at long wavelengths was extrapolated into the submillimeter regime using published fluxes from 6 cm to 1.3 mm (Churchwell et al. 1987; Garay et al. 1987; Felli et al. 1993; Zapata et al. 2004; Mundy et al. 1995; Bally et al. 1998b; Eisner & Carpenter 2006; Eisner et al. 2008). These data show a flat spectral dependence consistent with optically thin emission, $F_{\nu} \propto \nu^{0.1}$, but with a range, shown as grey scale, which we attribute to variability (Zapata et al. 2004) and possibly different amounts of background filtering. The turnover to optically thick emission occurs at longer wavelengths than shown and we have not attempted to model this. All but two $880 \mu\text{m}$ SMA fluxes exceed the extrapolated free-free emission indicating disk or background emission. A template disk spectrum, $F_{\nu} \propto \nu^2$ (Andrews & Williams 2005), is schematically plotted through the SMA data in Figure 3 to guide the eye.

The background at $880 \mu\text{m}$ was estimated by simulating the interferometric response to the

Johnstone & Bally (1999) SCUBA map. For each field, the SCUBA data were Fourier-transformed and sampled over the same uv -tracks as the observation, then inverted and cleaned to produce a spatially filtered map. The background flux at each disk position was then measured in the same manner as the observations themselves.

The dust-disk flux was determined by subtracting free-free and background contributions from the observed flux (Table 1). We found that 26 of our 28 detections had significant dust emission. Disk masses, and upper limits for the non-detections, were derived based on the standard relationship,

$$M_{\text{disk}} = \frac{F_{\text{dust}} d^2}{\kappa_{\nu} B_{\nu}(T)}, \quad (2)$$

where $d = 400 \text{ pc}$ is the distance to Orion (Sandstrom et al. 2007; Menten et al. 2007), $\kappa_{\nu} = 0.1(\nu/1000 \text{ GHz}) = 0.034 \text{ cm}^2 \text{ g}^{-1}$ is the dust grain opacity with an implicit gas-to-dust mass ratio of 100:1, and $B_{\nu}(T)$ is the Planck function at temperature $T = 20 \text{ K}$. We used the same dust opacity and temperature as the disk surveys of Taurus and ρ Ophiuchus by Andrews & Williams (2005, 2007a) since we wish to make a direct comparison with these studies, but revisit these assumptions in §4.

We also derived the mass sensitivity of the survey by determining the fraction of sources that could be detected at $\geq 3\sigma$ at each mass. We input disk masses and observed free-free emission, adding appropriate point sources to the SCUBA map, and simulating observations in the same manner as described above for the background contamination. Our survey is 100% complete for disk masses $\geq 0.0084 M_{\odot}$ and 85% complete for masses a factor of two lower.

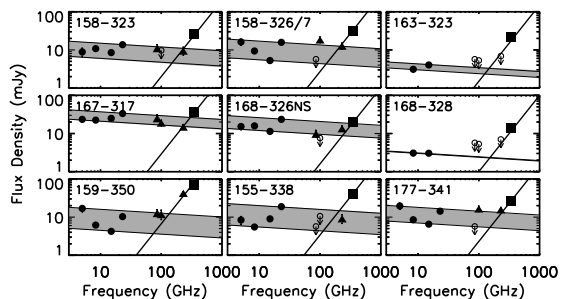


FIG. 3.— Spectral energy distributions for 9 proplyds detected at $\geq 3\sigma$ with the SMA at $880 \mu\text{m}$. The SMA measurements are represented by squares, millimeter observations by triangles and centimeter observations by circles. Open circles are upper limits from non-detections and uncertainties not shown are smaller than symbol sizes. The extrapolated range of optically thin free-free emission, $F_{\nu} \propto \nu^{-0.1}$, is overlaid in gray. A template to the disk emission, $F_{\nu} \propto \nu^2$, shows the relative contributions of the ionized gas and dust components.

3.2. Comparison with Taurus and ρ Ophiuchus

Having measured masses for a moderate sample of Trapezium Cluster disks, we can address how they compare with disks in Taurus and ρ Ophiuchus and assess the effect of environment on disk evolution. We use the results of the SCUBA surveys of Andrews & Williams (2005, 2007a) and consider only Class II disks as they

have ages $\sim 1 \text{ Myr}$, similar to those estimated for the Trapezium Cluster. The differential disk mass distributions for the three samples are plotted in Figure 4 with the same bins, $\Delta \log M_{\text{d}} = 2$, and with a start point that separates the complete and incomplete samples in the Trapezium Cluster.

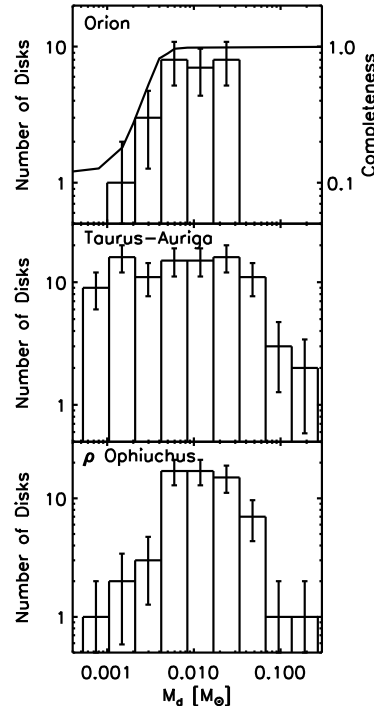


FIG. 4.— Differential disk mass distribution in Orion, Taurus and ρ Ophiuchus. The error bars for the distributions are \sqrt{N} . The fraction of disks that would be detected in our survey at each mass is indicated by the continuous line in the top panel. Binning begins at $0.0084 M_{\odot}$ to separate complete and incomplete samples. The number of disks per logarithmic mass bin is approximately constant for masses $0.004 - 0.034 M_{\odot}$ in all three regions but there are no disks with masses $> 0.034 M_{\odot}$ in Orion.

Figure 4 shows that the number of disks per logarithmic mass is approximately constant for the 3 bins spanning $0.004 - 0.034 M_{\odot}$ in each region but there are no Trapezium disks in the higher mass bins. This cannot be explained by observational biases, since such massive disks would be readily detectable in our observations. If the Trapezium disk mass distribution were similar to Taurus (or ρ Ophiuchus), we would expect 8 (4) disks with masses $> 0.034 M_{\odot}$ in our sample. With this expectation, the probability of detecting none is 0.03% (1.8%) respectively. Two-tailed Kolmogorov-Smirnov (KS) tests on the disk distributions above $0.0084 M_{\odot}$ for which all observations are fully complete, show that the Trapezium disk distribution is different from that in both Taurus and ρ Ophiuchus at $> 5\sigma$ significance. The difference remains significant if the disk luminosities are compared, and shows that the flux-mass conversion is not responsible for the observed discrepancy. We conclude that the disk mass distribution in the Orion Trapezium Cluster is truncated at high masses.

Eisner et al. (2008) also noted a lack of massive disks in the Trapezium Cluster from a larger scale but longer wavelength survey. We agree with their finding but

TABLE 1
 DISK FLUXES AND MASSES

Proplyd Name (a)	Field (b)	F_{obs} (mJy) (c)	rms (mJy) (d)	F_{ff} (mJy) (e)	F_{bg} (mJy) (f)	F_{dust} (mJy) (g)	M_{disk} ($10^{-2} M_{\odot}$) (h)
155-338	D	39.6	5.3	4.0–14.0	2.6	23.0	1.13 ± 0.34
158-323	B	25.5	2.4	4.3–11.5	-5.6	19.5	0.96 ± 0.21
158-326/7	B	31.9	2.4	4.0–12.0	-0.5	20.3	1.00 ± 0.19
159-350	D	69.8	5.3	3.2–11.0	0.3	58.4	2.86 ± 0.29
161-328	B	38.7	2.4	0.1–1.5	-1.2	38.4	1.88 ± 0.15
163-249	I	34.8	2.0	0.0	-1.6	36.4	1.78 ± 0.13
163-323	B	22.1	2.4	2.4–3.0	0.2	18.9	0.93 ± 0.15
167-317	B	37.2	2.4	14.5–25.5	-5.4	17.0	0.83 ± 0.18
168-328	B	13.7	2.4	1.9–2.5	1.0	10.3	0.50 ± 0.12
170-249	I	14.6	2.0	0.0–2.5	-0.6	12.6	0.62 ± 0.10
170-337	A	19.1	1.5	4.0–9.0	3.0	7.1	0.32 ± 0.08
171-340	A	46.4	1.5	0.0	-2.8	49.2	2.23 ± 0.08
174-236	I	25.2	2.0	0.0	2.9	22.2	1.09 ± 0.13
174-414	C	12.7	1.5	0.0	1.6	11.1	0.51 ± 0.09
175-355	A	9.4	1.5	0.0	-0.1	9.5	0.43 ± 0.11
176-543	G	15.8	1.7	0.0	-0.6	13.4	0.89 ± 0.09
177-341	A	26.9	1.5	5.0–13.0	-4.9	19.8	0.90 ± 0.07
182-413	C	13.3	1.5	0.0	-3.0	16.4	0.74 ± 0.07
183-419	C	6.2	1.5	0.0	0.2	6.1	0.28 ± 0.07
197-427	E	57.7	1.9	0.0	-1.5	59.3	2.72 ± 0.10
198-448	F	16.4	2.0	0.0	-2.9	19.3	0.94 ± 0.12
203-506/4	F	14.3	2.0	0.0	-2.9	17.2	0.84 ± 0.12
205-421	E	54.8	1.9	0.0	-1.7	56.5	2.59 ± 0.10
206-446	F	63.3	2.0	0.0	0.0	63.3	3.10 ± 0.12
218-339	H	6.9	0.9	0.0	0.0	6.6	0.34 ± 0.04
218-354	H	42.9	0.9	0.0	-0.9	48.1	2.10 ± 0.04

NOTE. — (a) Proplyd designation based on the nomenclature of O’Dell & Wen (1994). (b) Observed Field in Figure 1. (c) Integrated continuum flux density, corrected for SMA primary beam attenuation. (d) 1σ statistical error. (e) Range of extrapolated contribution of free–free emission at $880\mu\text{m}$. (f) Estimated flux contribution from cloud background. (g) Derived dust continuum flux from the disk. (h) Disk mass.

our results differ in the details. First, we generally detect significant $880\mu\text{m}$ emission only toward HST-identified disks. There are just two points in our 9 maps that exceed 5σ and are not coincident with a catalogued proplyd. In particular, we do not detect other known objects such as the infrared sources cataloged by Hillenbrand & Carpenter (2000). We suspect that at least some of the HC and MM sources in Eisner et al. (2008) are filtered small-scale background fluctuations despite their precaution in using localized measures of the noise. Second, the SEDs in Figure 3 show that several of the detections listed at 3 mm by Eisner & Carpenter (2006) and 1.3 mm by Eisner et al. (2008) are consistent with being free-free, rather than disk, emission. Although they attempted to separate contributions from dust and free-free emission, this process is much easier at shorter wavelengths. Further, we were more conservative, using a range to allow for variability in the radio emission. The difficulty in separating out the contributions from the ionized gas and the dust and, to a lesser extent, the cloud background, results in several significant discrepancies in individual disk mass determinations between our work and theirs.

4. DISCUSSION

We first address the flux-to-mass conversion in equation 2. Our prescription for the dust grain opacity, κ is from Beckwith et al. (1990) but its value depends on the grain composition and size distribution. Detailed models by Pollack et al. (1994) and Ossenkopf & Henning (1994) show that, excluding the diffuse ISM, the range in

$\kappa(1\text{ mm})$ is about a factor of 4. A low surface area to mass is required to explain the observed low maximum disk luminosity in the Trapezium Cluster. Throop & Bally (2005) have proposed that gas loss through photoevaporation promotes dust coagulation but since the former mainly occurs in the outer disk, it does not appear to be applicable to the many small disks detected here. However, given that there are several indications of significant grain growth in Taurus and ρ Ophiuchus Class II disks (Andrews & Williams 2005, 2007a), there is insufficient remaining leverage in κ to account for the lower disk luminosities in the Trapezium Cluster. Additional evidence against a large range in κ is the similarity of the Taurus and ρ Ophiuchus disk mass distributions (Andrews & Williams 2007a). We have assumed a low temperature, 20 K, derived from the average for Taurus disks (Andrews & Williams 2005) however, the high radiation field might significantly heat the Orion disks. But a higher temperature would reduce the inferred Trapezium Cluster disk masses yet further. The only remaining variable is the distance to the Trapezium, which has been securely determined from recent VLBI parallax observations (Menten et al. 2007; Sandstrom et al. 2007) and the small error cannot account for the luminosity difference. Finally, we note that different scalings do not change the shape of the distributions and our finding that the Trapezium Cluster disk mass distribution is truncated at its upper end.

The lack of massive disks in the Trapezium Cluster is in good agreement with theoretical models of disk

photoevaporation (Adams et al. 2004; Johnstone et al. 1998). Photoevaporation is thought to be the dominant external influence on disk evolution in the Trapezium Cluster as the rate of disk-disk encounters is low (Scally & Clarke 2001). The models predict that mass loss is highest for the largest disks because material at large radii is unbound to the embedded star and provides a greater surface area for photoevaporation. In contrast, the inner regions of the disk are gravitationally bound and can survive longer: while it takes only 2 Myr to erode disks down to 50 AU size scales, the dust and gas at smaller radii may survive external photoevaporation for > 10 Myr (Adams et al. 2004; Clarke 2007). Consequently, the largest disks, which are likely to be the most massive, would be quickly eroded to smaller radii and lower masses. The factor of ~ 3 reduction between the upper end of the Trapezium Cluster versus the Taurus and ρ Ophiuchus disk mass distributions corresponds to a reduction of 3 – 9 in radius for a power law surface density profile, $\Sigma(r) \sim r^{-p}$, with $p = 1 - 1.5$ (Andrews & Williams 2007b). If the Trapezium Cluster disks started out with initial properties similar to Taurus disks, which have a mean radii of 200 AU, range 100–700 AU and masses $0.01 - 0.17 M_{\odot}$ (Andrews & Williams 2007b), we would expect them to be eroded to scales < 70 AU and masses consistent with our survey. In fact, many of the Trapezium Cluster disks in our sample are unresolved by HST observations implying radii < 60 AU. And in the cases where the proplyds are seen in silhouette and the radius can be directly measured (Vicente & Alves 2005), we find that the largest disks, $R \sim 150$ AU, tend to be among the most massive, $M_d \sim 0.03 M_{\odot}$.

The truncation of the Trapezium Cluster disk mass distribution is a vivid illustration of the effect of nearby massive stars on disk evolution. The hostile environment, which includes both ionizing radiation and high density of stars, may preclude the formation of massive disks in their vicinity, or rapidly erode them after formation. Yet the effect of external photoevaporation on the inner, potentially planet-forming, regions of disks appears to be small. 12 of the disks in our sample exceed the MMSN and retain sufficient material to form planetary systems with masses like our own. Half of these (11% of the total sample) are unresolved with radii < 60 AU making them resistant to further photoevaporation. For comparison, $\sim 30\%$ of Taurus and ρ Ophiuchus Class II disks exceed a MMSN but these are generally larger than the Trapezium Cluster disks. A more meaningful comparison would be to estimate the fraction of disks containing a MMSN within their central 60 AU. This would

imply a total mass out to 200 AU of $\gtrsim 3$ MMSN, which is only found in about 13% of Taurus disks. The fraction of disks that appear capable of forming Solar Systems is similar in each region and lies between the $\sim 7\%$ detection rate of extrasolar planets in Doppler surveys (Marcy et al. 2008) and the $\sim 15\%$ debris disk fraction (Carpenter et al. 2008).

The formation of sub-Jupiter mass planets requires less material and may be possible for proplyds less massive than a MMSN. For example, 11 proplyds have sufficient mass ($\sim 1/3$ MMSN) and small sizes (< 60 AU) to potentially form Neptune. This fraction (20%) is a lower limit as our survey completeness drops rapidly for $M_d < 0.004 M_{\odot}$, but is on the lower end of a recent first estimate from the HARPS planet-search survey of $30\% \pm 10\%$ (Mayor et al. 2009).

5. SUMMARY

Our SMA survey of the Orion Trapezium Cluster detected 28 out of 55 HST-identified disks (“proplyds”) at $880 \mu\text{m}$ due to its combination of high sensitivity and resolution. We carried out a careful analysis of the disk SED from centimeter to submillimeter wavelengths and of the interferometric response to the cloud background to calculate the dust flux from each disk. We then determined dust masses for 26 disks and show the number of disks per logarithmic mass interval is approximately constant over almost a decade in mass between $0.004 - 0.034 M_{\odot}$, similar to Class II disks in both Taurus and ρ Ophiuchus. Extrapolating from these low mass star forming regions, we would have expected several disks with masses greater than the maximum in our survey, $0.034 M_{\odot}$. The truncation of the Trapezium Cluster disk mass distribution is likely due to photoevaporation of the outer disks by the O6 star, θ^1 Ori C, from an initial disk distribution similar to Taurus.

Six of the 55 disks exceed the MMSN and have radii < 60 AU, which is similar to the inferred initial conditions of the Solar System, whose sharp edge at ~ 50 AU may also be a product of photoevaporation (Jewitt et al. 1998; Trujillo, Jewitt, Luu 2001; Allen et al. 2001). We conclude that disks with the potential to form Solar Systems are no less likely in Orion than in dark clouds without massive stars.

This work is supported by the NSF through grant AST06-07710. We are grateful to David Jewitt, Michael Liu, Sean Andrews, and David Wilner for their comments.

REFERENCES

- Adams, F. C., Hollenbach, D., Laughlin, G., Gorti, U. 2004, ApJ, 611, 360
 Allen, R. L., Bernstein, G. M. & Malhotra, R. 2001, ApJ, 549, L241
 Andrews, S. M., & Williams, J. P. 2005, ApJ, 631, 1134
 Andrews, S. M., & Williams, J. P. 2007, ApJ, 671, 1800
 Andrews, S. M., & Williams, J. P. 2007, ApJ, 659, 705
 Bally, J., O’Dell, C.R. & McCaughrean, M. J. 2000, AJ, 119, 2919
 Bally, J., Testi, L., Sargent, A., Carlstrom, J. 1998, AJ, 116, 854
 Bally, J., Sutherland, R. S., Devine, D., Johnstone, D. 1998, AJ, 116, 293
 Beckwith, S. V. W., Sargent, A. I., Chini, R. S., Guesten, R. 1990, AJ, 99, 924
 Carpenter, J. M., et al. 2008, arXiv:0810.1003
 Churchwell, E., Wood, D. O. S., Felli, M., Massi, M. 1987, ApJ, 321, 516
 Clarke, C.J 2007, MNRAS, 376, 1350
 Eisner, J.A. & Carpenter, J.M. 2006, ApJ, 641, 1162
 Eisner, J.A., Plambeck, R.L., Carpenter, J.M., Corder, S.A. & Wilner, D. 2006, ApJ, 683, 304
 Felli, M., Churchwell, E., Wilson, T. L., Taylor, G. B. 1993, A&AS, 98, 137
 Garay, G., Moran, J. M., Reid, M. J. 1987, ApJ, 314, 535
 Henney, W. J. & O’Dell, C. R. 1999, AJ, 118, 2350
 Hillenbrand, L. A. 1997, AJ, 113, 1733
 Hillenbrand, L.A. & Carpenter, J. M. 2000, ApJ, 540, 236
 Jewitt, D.C., Luu, J. & Trujillo, C. 1998, AJ, 115, 2125

- Johnstone, D., Hollenbach, D. & Bally, J. 1998, ApJ, 499, 758
Johnstone, D. & Bally, J. 1999, ApJL, 510, L49
Lada, C. J. & Lada, E. A. 2003, ARAA, 41, 57
Marcy, G. W., et al. 2008, Physica Scripta Volume T, 130, 014001
Mayor, M., et al. 2009, A&A, 493, 639
McCaughrean, M. J., et al. 1998, ApJ, 492, L157
McCullough, P. R., Fugate, R. Q., Christou, J. C., Ellerbroek,
B. L., Higgins, C. H., Spinhirne, J. M., Cleis, R. A., & Moroney,
J. F. 1995, ApJ, 438, 394
Menten, K. M., Reid, M. J., Forbrich, J., & Brunthaler, A. 2007,
A&A, 474, 515
Mundy, L. G., Looney, L. W., Lada, E. A. 1995, ApJL, 452, L137
O'Dell, C.R. & Wen, Z. 1994, ApJ, 436, 194
O'Dell, C.R. & Wong, K. 1996, AJ, 111, 846
Ossenkopf, V., & Henning, T. 1994, A&A, 291, 943
Pollack, J. B., Hollenbach, D., Beckwith, S., Simonelli, D. P.,
Roush, T., & Fong, W. 1994, ApJ, 421, 615
Sandstrom, K. M., Peek, J. E. G., Bower, G. C., Bolatto, A. D., &
Plambeck, R. L. 2007, ApJ, 667, 1161
Sclally, A. & Clarke, C.J. 2001, MNRAS, 325, 449
Throop, H. B., & Bally, J. 2005, ApJ, 623, L149
Trujillo, C., Jewitt, D.C. & Luu, J. 2001, AJ, 122, 457
Vicente, S.M. & Alves, J. 2005, A&A, 441, 195
Weidenschilling, S. J. A&SS, 1977, 51, 153
Williams, J. P., Andrews, S. M., & Wilner, D. J. 2005, ApJ, 634,
495
Zapata, L. A., Rodriguez, L. F., Kurtz, S. E., O'Dell, C. R. 2004,
AJ, 127, 2252